Effects of chloride ion concentration on the corrosion behavior of the AA2198-T8 alloy

Caruline de Souza Carvalho MACHADO[1], Rejane Maria da SILVA[1], João Victor de Sousa ARAUJO[1], Uyime DONATUS[1], Mariana Xavier MILAGRE[1], Rafael Emil KLUMPP[1], Jesualdo L. ROSSI[1], Isolda COSTA[1]

[1]IPEN-CNEN/SP, São Paulo, Brasil, carulinemachado@yahoo.com.br
[1]IPEN-CNEN/SP, São Paulo, Brasil, rejanep2silva@gmail.com
[1]IPEN-CNEN/SP, São Paulo, Brasil, joão-neutron@hotmail.com
[1]IPEN-CNEN/SP, São Paulo, Brasil, uyimedonatus@yahoo.com.br
[1]IPEN-CNEN/SP, São Paulo, Brasil, marianamilagre@yahoo.com.br
[1]IPEN-CNEN/SP, São Paulo, Brasil, rafahemil@hotmail.com
[1]IPEN-CNEN/SP, São Paulo, Brasil, jelrossi@ipen.br
[1]IPEN-CNEN/SP, São Paulo, Brasil, icosta@ipen.br

Abstract

In this work, the influence of chloride ions concentration on the corrosion behavior of the AA2198-T8 alloy was evaluated. Immersion test and electrochemical analyses were performed in sodium chloride solutions of three concentrations, 0.001 mol L^{-1}, 0.005 mol L^{-1} and 0.01 mol L^{-1}. The results showed that the AA2198-T8 alloy was susceptible to localized corrosion (LC) and to severe localized corrosion (SLC) in all conditions investigated. The electrochemical results obtained by open circuit potential measurements, cyclic voltammetry and potentiodynamic polarization curves were associated with the corroded microstructure of the alloy. Although electrochemical techniques allowed differentiating the corrosion resistance as a function of chloride concentration, the result was strongly influenced by the corroded/uncorroded area ratio related to the SLC.

Keywords: Aluminum alloy; severe localized corrosion; electrochemical techniques.

Introduction

Al-Cu-Li alloys have a great potential for applications in aeronautical industry due to their low density and good mechanical properties, however, localized corrosion is a characteristic problem concerning these alloys [1–4]. This results from their microstructure, which is composed by several phases (constituent particles, precipitates) presenting electrochemical properties different from those of the matrix [5,6]. Constituent particles present micrometric sizes and are associated to localized corrosion (LC) while nanometeric precipitates are related to hardening of the alloy. The main precipitate is Al-Cu-Li alloys which results in decreased corrosion resistance is the T1 phase (Al_2CuLi). This has been associated with a strong attack of the allou, also known in literature as severe localized corrosion (SLC). SLC differs from the LC induced by constituent particles because the area of attack at the surface is larger in the SLC compared to LC. Moreover, SLC presents particular features, such as rings of corrosion products, cathodically protected areas surrounding the SLC and hydrogen gas evolution at areas surrounding the pit mouth [3–5].

Corrosion of aluminum alloys is not uniform and, consequently, the electrochemical results measured by global electrochemical techniques represent an average of surface events. This is particularly relevant for SLC, which is associated with higher current densities compared to LC [3]. The number of SLC sites nucleated on the exposed surface during immersion tests can vary, as well as the kinetics of pit evolution, resulting in different magnitudes of penetration and size of protected area. Consequently, the anodic/cathodic ratio, represented by the attacked/unattacked areas, has an important role during electrochemical measurements. Since the oxide film around the sites of SLC usually remains preserved, the use of environments of low concentration seems adequate to study this kind of alloys, once it allows monitoring the slight modifications on the surface due to corrosion attack.

In this work, a relation between chloride concentration and the corroded area in the AA2198-T8 alloy was established with the aim of correlating microstructure with the corrosion resistance of this alloy by using electrochemical measurements (open circuit potential, polarization curves and cyclic voltammetry) and immersion tests.

Experimental

Microstructural characterization

4 mm thick plate of AA2198-T8 alloy (3.32 wt% Cu, 0.96 wt% Li, 0.31 wt% Mg, 0.26 wt% Ag, 0.51 wt% Zr, 0.05 wt% Fe, 0.04 wt% Si, 0.04 wt% Zn, 0.02 Mn) was used in this study. The constituent particles in the AA2198-T8 were characterized after surface preparation by sequential polishing using SiC paper (up to #4000) and diamond pastes of 3 μm and 1 μm. Following surface preparation, the specimens were cleaned in acetone, rinsed in deionized water and dried under a cool air stream. Semi-quantitative analyses of 150 micrometric precipitates were performed by EDX in order to estimate their chemical composition, using JSM-6701F field emission gun scanning electron microscope (FEG-SEM). Specimens for transmission electron microscopy (TEM) were obtained by cutting 3

mm diameter discs from the alloy. The cut samples were mechanically thinned and prepared by double-jet electro-polishing with a solution comprising 20% HNO_3 in methanol at 25 V and -30 °C. TEM images were obtained in a JEOL 2100F microscope.

Corrosion evaluation

Immersion test was performed by exposing the samples (surface finishing corresponding to polish with 1 μm diamond suspension) to naturally aerated solution. Three concentrations of NaCl solution were used: 0.01 mol L^{-1}; 0.005 mol L^{-1} and 0.001 mol L^{-1}. The samples were removed from the test solution after 4 h, 12 h, and 24 h; rinsed with deionized water and dried under cold air stream. Subsequently, the exposed surfaces were observed by optical microscopy. Electrochemical measurements were carried out in the solutions of various chloride concentrations. An Ag/AgCl (KCl saturated) electrode was used as reference, a platinum wire as counter electrode and the AA2198-T8 alloy as working electrode. All the measurements were performed after surface preparation (grinding and polishing up to 1 μm diamond finishing). The area exposed to test solutions was 1 cm^2. Open circuit potential (OCP) meaurements were carried out in the test solution for 24h. Polarization tests were carried out after 15 min of exposure to the test solutions, from -0.02 V vs OCP to 1 V at a scan rate of 0.5 mV s^{-1}. Subsequently, cyclic voltammetry was carried out from -1.1 V to -0.1 V, at a scan rate of 10 mV s^{-1} totalizing 2 cycles.

Results and Discussion

Microstructural Characterization

Different from the micrometric particles, the nanometric precipitates are intentionally formed during thermomechanical or heating treatments in order to increase the alloy strength. Figure 2 shows a TEM micrograph of the AA2198-T8 allooy, which revealed grains with high density of thin hexagonal plates, which are identified as T1 phase (Al2CuLi). T1 phase is the predominant strengthening phase in Al-Cu-Li alloys, however, due to its high electrochemical activity, it is also associated with severe localized corrosion (SLC) [3–5,10–12]. Compared with the micrometric particles, in the AA2198-T8 alloy, the T1 phase presents a homogeneous distribution inside the grains. Attack propagation is eased in the areas of high T1 phase concentration, and, in the case of the alloy of this study it may result in grain consumption.(a) shows the constituent particles on the surface of AA2198-T8 alloy. These are aligned in the mechanical working direction. These particles are formed during alloy solidification from impurities or elements of low solubility in aluminium [7]. EDX analysis (Different from the micrometric particles, the nanometric precipitates are intentionally formed during thermomechanical or heating treatments in order to increase the alloy strength. Figure 2 shows a TEM micrograph of the AA2198-T8 allooy, which revealed grains with high density of thin hexagonal plates, which are identified as T1 phase (Al2CuLi). T1 phase is the predominant strengthening phase in Al-

Cu-Li alloys, however, due to its high electrochemical activity, it is also associated with severe localized corrosion (SLC) [3–5,10–12]. Compared with the micrometric particles, in the AA2198-T8 alloy, the T1 phase presents a homogeneous distribution inside the grains. Attack propagation is eased in the areas of high T1 phase concentration, and, in the case of the alloy of this study it may result in grain consumption.(b)) revealed that they are mainly composed of Al, Fe and Cu and are enriched in these two last elements (Table 1). The constituent particles are cathodic to the matrix, since they are enriched in Cu. Consequently, localized attack at the matrix surrounding these particles has been observed when they are exposed to corrosive environments [4,8,9].

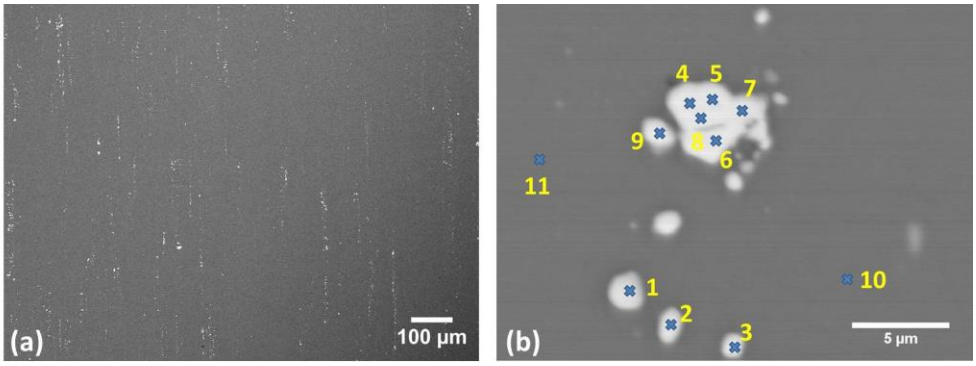

Figure 1 – Surface of the AA2198-T8 alloy showing (a) micrometric constituent particles aligned in the mechanical working direction and (b) points analysed by EDX.

Table 1 - EDX analysis from micrometric constituent particles in the AA2198-T8 alloy and from the alloy matrix.

	Al-K	**Fe-K**	**Cu-K**	**Cu/Fe**
1	72.8	7.1	20.1	2.8
2	71.5	7.3	21.3	2.9
3	73.8	6.8	19.4	2.9
4	65.3	9.5	25.2	2.7
5	60.7	11.0	28.4	2.6
6	55.9	12.7	31.4	2.5
7	62.3	10.7	27.1	2.5
8	59.3	11.3	29.4	2.6
9	69.3	8.2	22.5	2.7
10	96.5	0.1	3.4	34
11	96.4	0.1	3.6	36

Different from the micrometric particles, the nanometric precipitates are intentionally formed during thermomechanical or heating treatments in order to increase the alloy strength. Figure 2 shows a TEM micrograph of the AA2198-T8 allooy, which revealed grains with high density of thin hexagonal plates, which are identified as T1 phase (Al_2CuLi). T1 phase is the predominant strengthening phase in Al-Cu-Li alloys, however,

due to its high electrochemical activity, it is also associated with severe localized corrosion (SLC) [3–5,10–12]. Compared with the micrometric particles, in the AA2198-T8 alloy, the T1 phase presents a homogeneous distribution inside the grains. Attack propagation is eased in the areas of high T1 phase concentration, and, in the case of the alloy of this study it may result in grain consumption.

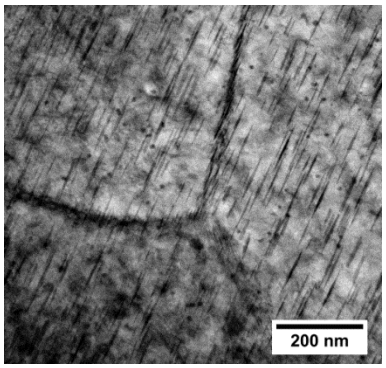

Figure 2 - TEM image of the AA2198-T8 alloy showing high density of thin nanometric plates inside the grains.

Immersion test

Figure 3 compares the evolution of the exposed surfaces during 24h of immersion in the solutions of various chloride concentrations used in this study. The surface area attacked in all solutions showed the high susceptibility of the studied alloy to localized corrosion. The development of corrosion shows that the electrochemical activity of the phases present differs from the matrix [6,13]. Surface observation allows identifying different kinds of localized attack according to their characteristics, and these were classified in severe (SLC) and not-severe localized corrosion (LC). Several studies [3–5,10,11,14] showed that SLC in this kind of alloys is associated with the high activity of T1 phase [6], which was abundant in the alloy (Figure 2). As already mention, this type of attack results in a cathodically protected area around the central pit and hydrogen gas evolution around the active sites [3–5,9,15]. On the other hand, localized corrosion (LC) is associated with micrometric particles that, in the case if this study are cathodic to the matrix (Different from the micrometric particles, the nanometric precipitates are intentionally formed during thermomechanical or heating treatments in order to increase the alloy strength. Figure 2 shows a TEM micrograph of the AA2198-T8 allooy, which revealed grains with high density of thin hexagonal plates, which are identified as T1 phase (Al2CuLi). T1 phase is the predominant strengthening phase in Al-Cu-Li alloys, however, due to its high electrochemical activity, it is also associated with severe localized corrosion (SLC) [3–5,10–12]. Compared with the micrometric particles, in the AA2198-T8 alloy, the T1 phase presents a homogeneous distribution inside the grains. Attack propagation is eased in the areas of high T1 phase concentration, and, in the case of the alloy of this study it may result in grain consumption.). These were responsible for the surface darkening due to the corrosion products formed. A layer of adherent corrosion products might decrease the

electrochemical activity at the surface, since it acts as a physical barrier between the surface and the environment.

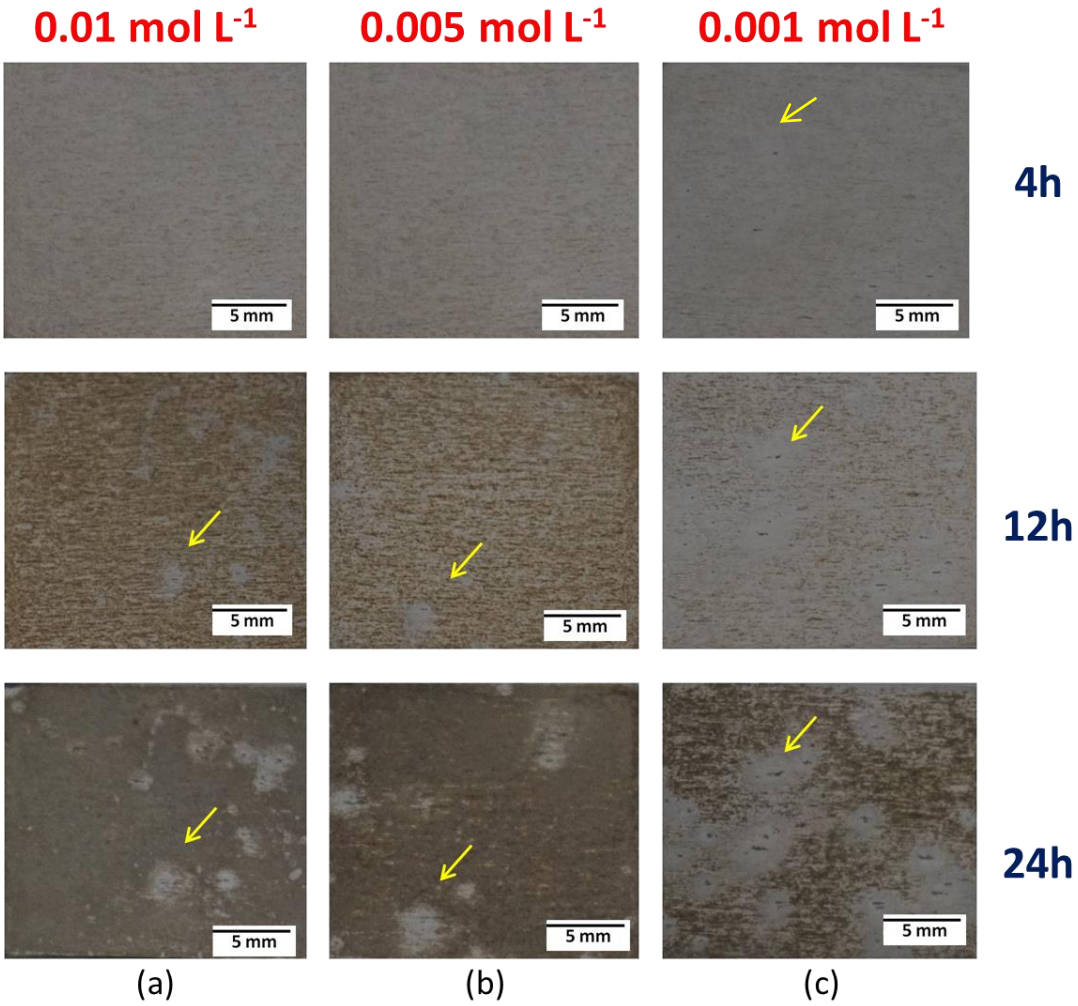

Figure 3 - Evolution of the AA2198-T8 surface during 24h of immersion in sodium chloride solutions with (a) 0.01 mol L^{-1}; (b) 0.05 mol L^{-1}; (c) 0.001 mol L^{-1} of NaCl.

It is expected that the degree of corrosion increases with the chloride concentration in solution, since chloride stimulates oxide film attack and, consequently, metal dissolution [16,17]. In this sense, Figure 3 suggests that the increase in chloride concentration results in increased areas of attack. However, in Al-Cu-Li alloys, the attack related to greater damage is SLC and the samples exposed to the solution of lowest chloride concentration were the ones where SLC sites nucleated first (after 4h of exposure) and the areas affected by SLC were the largest. A comparison of the ratio between the preserved area and the corroded ones shows that larger areas were attacked in the most diluted solution. It is interesting to note that in the solution with 0.005 mol L^{-1} of NaCl the evolution of corrosion was similar to that observed for the sample exposed to 0.01 mol L^{-1} of NaCl and had no similarity to that in the 0.001 mol L^{-1} of NaCl. This observation is supported by surface observation by optical microscopy, as shown in Figure 4.

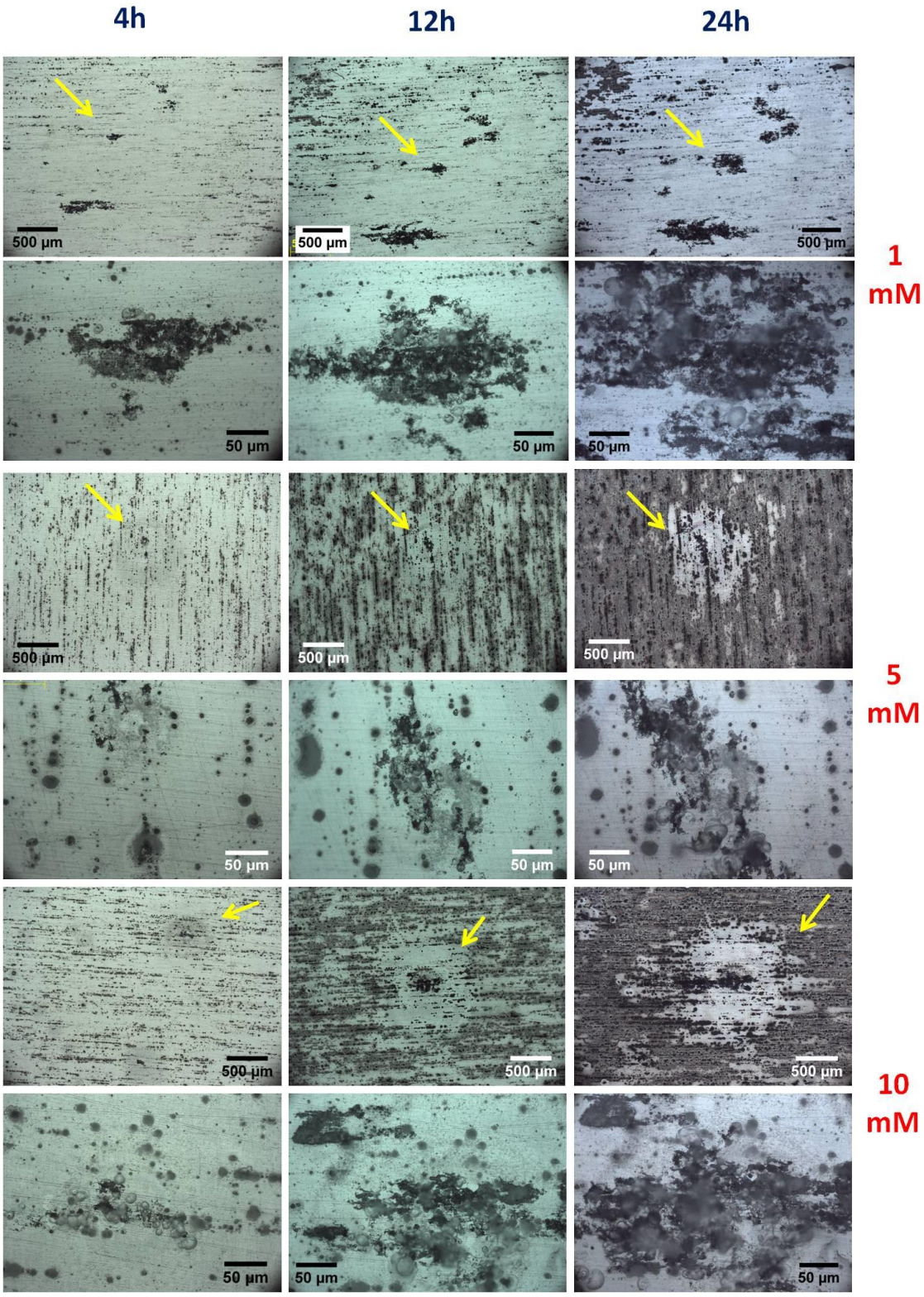

Figure 4 - Evolution of the AA2198-T8 surface during 24h of immersion in solution with (a) 0.01 mol L^{-1}; (b) 0.05 mol L^{-1}; and (c) 0.001 mol L^{-1} of NaCl.

The images of greater magnification in Figure 4 evidenced that the extent of severe attack was greater in the sample exposed to the least concentrated solution. This result shows that the chloride ions concentration in solution plays an important role in the kinetics and development of severe attack in solution of very low aggressiveness. These findings show that exposure of this kind of alloys to solutions of low corrosiveness might lead to unexpected results with increased areas of attack related to solutions of lower corrosiveness. It might also be inferred that, due to the larger cathodic protected area, the penetration of attack is deeper in the sample exposed to the solution of lower concentration.

Global Electrochemical Measurements

Figure 5 compares the open circuit potential (OCP) variation with time of immersion of the AA2198-T8 alloy during 24 h of exposure to the chloride solutions. The stability of the oxide film depends on the relative rates of the two opposing processes, repassivation and dissolution of the film [17]. Comparing the OCP during the initial periods of immersion, the OCP values of the samples exposed to the 0.001 mol L^{-1} NaCl solutions presented the highest potentials what is mainly due to the highest ohmic drop related to this solution and the preservation of the oxide film favored in solution of low concentration, which is in agreement with what was observed in the immersion test. However, in the 0.01 mol L^{-1} NaCl solution it rapidly decreased and them oscillated around -0.56 These oscillations in OCP occur independently of the concentration of chloride used and are related to the localized attack of the oxide film by the chlorides ions [9]. The decrease in potential is related to passive film attack, while the increase in potential is related to reform of the oxide film (repassivation).

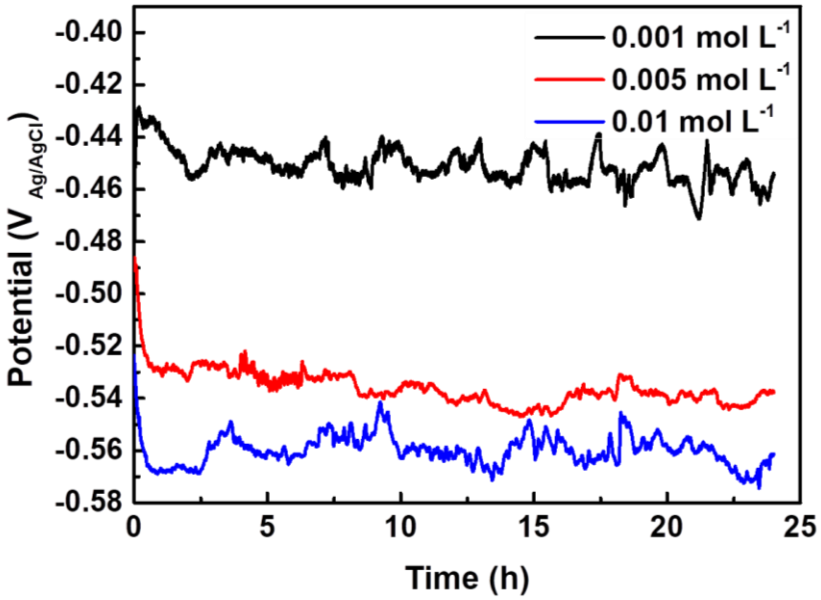

Figure 5 - Open circuit potential variation with time of exposure to 0.001 mol L^{-1}; 0.05 mol L^{-1} and 0.01 mol L^{-1} NaCl solutions.

The cathodic polarization curves of the AA2198-T8 alloy are shown in Figure 6. During the polarization, the cathodic reactions are favored and these occur preferentially on the micrometric (Cu, Fe enriched particles). The curves show a diffusion-controlled corrosion process, with a limiting current that increases with the chloride ion concentration, although all values are in the range of $2x10^{-6}$ A/cm² to $6x10^{-6}$ A/cm². The limiting current increased with solution concentration but only small variations were seen, but it may be due to the solubility of the oxygen, which is dependent on the concentration of chloride. Thus, the cathodic polarization does not allow to clearly differentiating the effect of the solution concentration on these alloys.

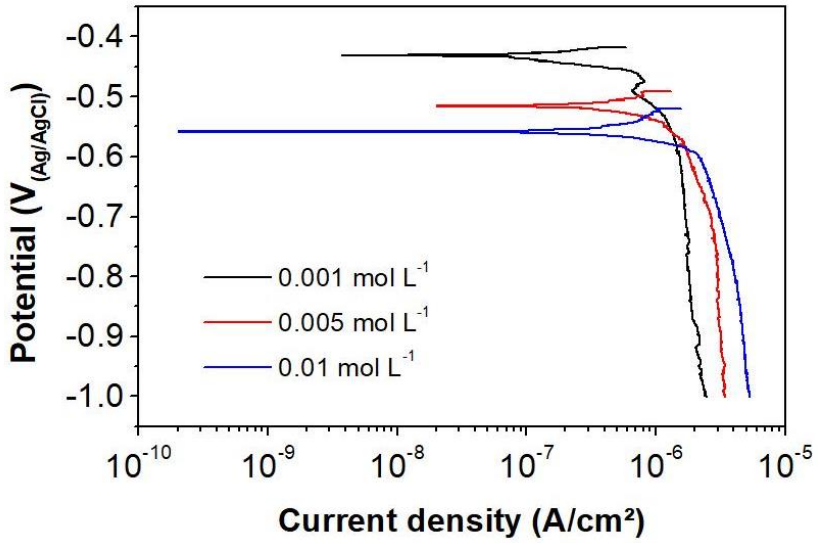

Figure 6 - Cathodic polarization curves for the AA2198-T8 alloy exposed to 0.001 mol L^{-1}; 0.05 mol L^{-1}; 0.01 mol L^{-1} of NaCl solutions.

Since the anodic polarization curves are related to dissolution of the passive film, significant differences could be observed among the solutions tested (Figure 7). Only the curve corresponding to the 0.001 mol L^{-1} NaCl solution showed a pseudo-passive behavior, whereas in the other concentrations, there is no indication of resistance to the anodic reactions of metal dissolution. The pseudo-passive behavior is explained by the remaining of oxide film on large areas of the surface. The observation of localized corrosion developing under open circuit potential conditions shows that the anodic polarization curve in the solution of lowest concentration proves that it is a pseudo-passive behavior. For an overpotential of -0.1 V, the comparison of the current densities for the three solutions shows that, for the 0.001 mol L^{-1} NaCl solution, the value is in the order of 10^{-7} A / cm², while for the other solution of higher chloride concentrations is in the range of 10^{-4} A / cm². Ambat et al [17] also observed that the increase in the concentration of chloride ions shifts the anodic curve to higher values of current density.

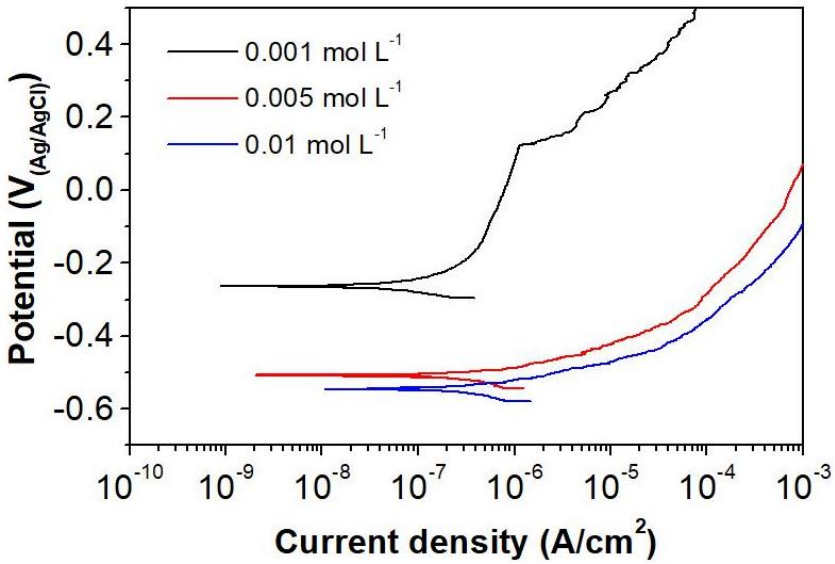

Figure 7 - Anodic polarization curves for the AA2198-T8 alloy exposed to 0.001 mol L^{-1}; 0.005 mol L^{-1}; 0.01 mol L^{-1} NaCl solutions.

After anodic polarization the attacked surface by oxidation reactions were compared, Figure 8. The main type of attack of the surfaces in both solutions was the SLC and the proportion of attacked regions in the solution of highest concentration was significantly higher than in the solution of lowest concentration. At higher magnification images it was seen that it led to grain consumption.

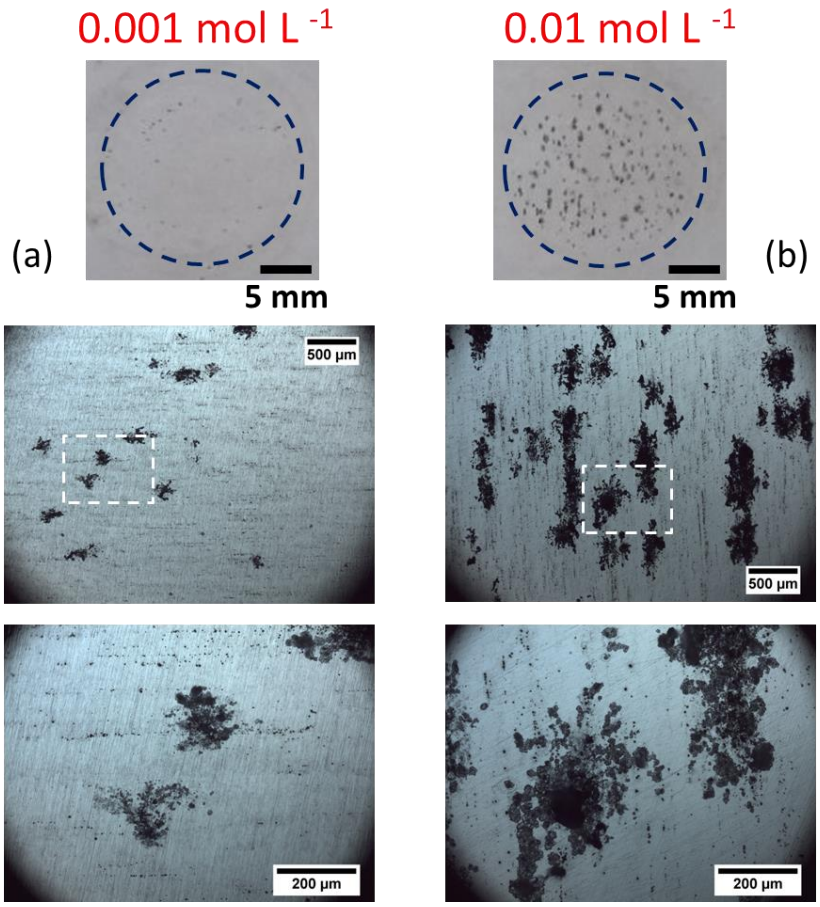

Figure 8 - Surface of the AA2198-T8 alloy after anodic polarization in (a) 0.001 mol L^{-1} and (b) 0.01 mol L^{-1} NaCl solutions.

The preservation of passive film on large areas of the surface in the specimens exposed to 0.001 mol L^{-1} NaCl solution was confirmed by cyclic voltammetry (Figure 9). The smallest hysteresis area was obtained for the lowest chloride concentration solution in contrast with the solution with the highest concentration (0.01 mol L^{-1} NaCl) and highest hysteresis area. In fact, a breakdown potential was not found in the 0.001 mol L^{-1} NaCl solution, while it was clearly identified in the solutions of higher concentrations. Also the highest current density after breakdown was related to the highest concentration solution.

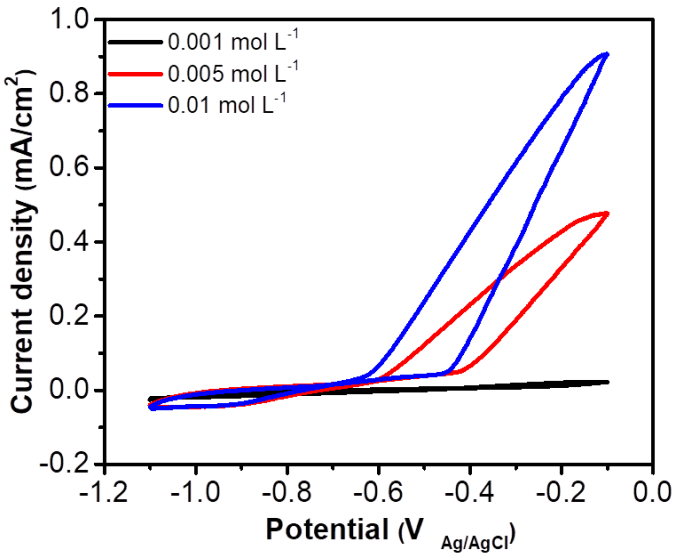

Figure 9 - Cyclic voltammetry curves from AA2198-T8 alloy exposed to 0.001 mol L^{-1}; 0.005 mol L^{-1}; 0.01 mol L^{-1} NaCl solutions.

Conclusions

Immersion tests of the AA2198-T8 alloy in solutions of three different concentrations of chloride showed that in solutions of low ions concentration, severe localized corrosion sites developed faster and in higher amounts which are likely due to the high resistivity of the solution between anodic and cathodic sites. A pseudo-passive behavior was related to the solution of lowest concentration. In summary, improved corrosion resistance was related to the sample exposed to the lowest concentration solution. The highest potential and the large oscillations in the solution of lowest chloride concentration along the 24h of test shows that localized attack is favored in this solution and it is continued for long periods of test. It is noteworthy that the global electrochemical tests do not differentiate the response of LC and SLC, consequently, to study this kind of alloy, localized techniques are necessary to better understanding the mechanism of corrosion.

Acknowledgments

The authors acknowledge to FAPESP (Proc. 2013/13235-6) and CAPES (Capes/Cofecub No806-14) for financial support for this work. The authors are thankful also to CAPES PROEX for the grants of Caruline de S. C. Machado (88882.333459/2019-01) and Mariana X. Milagre (88882.333479/ 2019-01). Thanks are also due to Dr. Naga Vishnu V. Mogili and Victor Ferrinho Pereira from Brazilian Nanotechnology National Laboratory/Brazilian Center for Research in Energy and Materials (LNNano/CNPEM) for TEM analysis and the weldment of alloy.

References

[1] T. Dursun, C. Soutis, Recent developments in advanced aircraft aluminium alloys, Mater. Des. 56 (2014) 862–871. doi:10.1016/j.matdes.2013.12.002.

[2] I.J. Polmear, Aluminium Alloys--A Century of Age Hardening, Mater. Forum. 28 (2004) 1–14. doi:7F6104775CD4BCE9E9D087602166B700.

[3] J.V. de S. Araujo, U. Donatus, F.M. Queiroz, M. Terada, M.X. Milagre, M. Cavalieri, I. Costa, On the severe localized corrosion susceptibility of the AA2198-T851 alloy, Corros. Sci. 133 (2018) 132–140. doi:10.1016/j.corsci.2018.01.028.

[4] U. Donatus, M. Terada, C. Ramirez, F. Martins, A. Fatima, S. Bugarin, I. Costa, On the AA2198-T851 alloy microstructure and its correlation with localized corrosion behaviour, 131 (2018) 300–309. doi:10.1016/j.corsci.2017.12.001.

[5] Y. Ma, X. Zhou, W. Huang, G.E. Thompson, X. Zhang, C. Luo, Z. Sun, Localized corrosion in AA2099-T83 aluminum-lithium alloy: The role of intermetallic particles, Mater. Chem. Phys. 161 (2015) 201–210. doi:10.1016/j.matchemphys.2015.05.037.

[6] R.G. Buchheit, A Compilation of Corrosion Potentials Reported for Intermetallic Phases in Aluminum Alloys, J. Electrochem. Soc. 142 (1995) 3994. doi:10.1149/1.2048447.

[7] N.E. Prasad, T.R. Ramachandran, Phase Diagrams and Phase Reactions in Al-Li Alloys, Elsevier Inc., 2013. doi:10.1016/B978-0-12-401698-9.00003-3.

[8] A.E. Hughes, N. Birbilis, J.M.C. Mol, S.J. Garcia, X. Zhou, G.E. Thompson, High Strength Al-Alloys: Microstructure, Corrosion and Principles of Protection, in: Z. Ahmad (Ed.), Recent Trends Process. Degrad. Alum. Alloy., Intech, Rijeka, 2011: pp. 223–262. doi:10.5772/18766.

[9] M.X. Milagre, U. Donatus, C.S.C. Machado, J.V. de S. Araujo, R.M.P. Silva, B.V.G. De Viveiros, I. Costa, R. Maria, P. Silva, B.V.G. De Viveiros, A. Astarita, I. Costa, Comparison of the corrosion resistance of an Al – Cu alloy and an Al – Cu – Li alloy, Corros. Eng. Sci. Technol. 0 (2019) 1–11. doi:10.1080/1478422X.2019.1605472.

[10] Y. long MA, X. rong ZHOU, X. min MENG, W. jiu HUANG, Y. LIAO, X. li CHEN, Y. nan YI, X. xin ZHANG, G.E. THOMPSON, Influence of thermomechanical treatments on localized corrosion susceptibility and propagation mechanism of AA2099 Al–Li alloy, Trans. Nonferrous Met. Soc. China (English Ed. 26 (2016) 1472–1481. doi:10.1016/S1003-6326(16)64252-8.

[11] J.V. de S. Araujo, C. de S.C. Milagre, Mariana Xavier Machado, I. Queiroz, Fernanda Martins Costa, Estudo da influência dos tratamentos termomecânicos T8 e T851 na microestrutura e na resistência à corrosão da liga AA2198, Corrosão & Proteção. 63 (2018) 32–44.

[12] M.X. Milagre, N. V. Mogili, U. Donatus, R.A.R. Giorjão, M. Terada, J.V.S. Araujo, C.S.C. Machado, I. Costa, On the microstructure characterization of the AA2098-T351 alloy welded by FSW, Mater. Charact. 140 (2018) 233–246. doi:10.1016/j.matchar.2018.04.015.

[13] N. Birbilis, R.G. Buchheit, Electrochemical Characteristics of Intermetallic Phases in Aluminum Alloys, J. Electrochem. Soc. 152 (2005) B140. doi:10.1149/1.1869984.

[14] C. de S.C. Machado, U. Donatus, R.A.R. Giorjão, V.F. Pereira, M.X. Milagre, R.E. Klumpp, J.V. de S. Araujo, N.V. Mogili, I. Costa, Corrosion behavior of AA2198-T8 friction stir welded alloy, in: Proc. Eur. Corros. Congr., 2018: p. 26.

[15] Y. long MA, X. rong ZHOU, X. min MENG, W. jiu HUANG, Y. LIAO, X. li CHEN, Y. nan YI, X. xin ZHANG, G.E. THOMPSON, Influence of thermomechanical treatments on localized corrosion susceptibility and propagation mechanism of AA2099 Al–Li alloy, Trans. Nonferrous Met. Soc. China (English Ed. 26 (2016) 1472–1481. doi:10.1016/S1003-6326(16)64252-8.

[16] B. Chen, C.H. Li, S.C. He, X.L. Li, C. Lu, Corrosion behavior of 2099 Al-Li alloy in NaCl aqueous solution, J. Mater. Res. 29 (2014) 1344–1353. doi:10.1557/jmr.2014.121.

[17] R. Ambat, E.S. Dwarakadasa, Studies on the influence of chloride ion and pH on the electrochemical behaviour of aluminium alloys 8090 and 2014, J. Appl. Electrochem. 24 (1994) 911–916. doi:10.1007/BF00348781.